Suppression of hydraulic transients for desalination plants based on active control synthesis

Bui Duc Hong Phuc, Sam-Sang You, Hwan-Seong Kim and Sang-Do Lee

ABSTRACT

This paper proposes a control strategy to stabilize a reverse osmosis desalination system against hydraulic shocks with enhancing productivity and sustainability. First, the effects of hydraulic transients on water quality have been reviewed. The transient waves are approximated by sinusoidal functions so that their effects are incorporated into the controlled system as external disturbances. Next, the active control is implemented based on the adaptive super-twisting (STW) sliding mode control (SMC) algorithms. Then, the robust performance is guaranteed whenever the sliding variables reach the sliding surfaces in finite time despite disturbances. The STW SMC scheme is to eliminate the chattering problems for protecting the valves and to improve the convergence precision for water production. The control gains are adaptable to enable formation of an effective controller for dealing with large disturbances such as water hammer during desalination process. The simulation results reveal the superior performances on controlling water product, while eliminating shock waves. Especially, the effect of hydraulic shocks has been dramatically attenuated, hence the plant components are protected to avoid fracture. Finally, the robust stability and performance of the desalination plants are guaranteed against large disturbances to ensure the population with quality water as well as system sustainability.

Key words | hydraulic transients, reverse osmosis, sliding mode control, water hammer, water quality

Bui Duc Hong Phuc
Department of Mechanical Engineering,
University of Tulsa,
Tulsa, OK 74104,
USA

Sam-Sang You (corresponding author)
Division of Mechanical Engineering,
Korea Maritime and Ocean University,
Busan 49112,
South Korea
E-mail: *ssyou@kmou.ac.kr*

Hwan-Seong Kim
Division of Logistics,
Korea Maritime and Ocean University,
Busan 49112,
South Korea

Sang-Do Lee
Division of Navigation and Information Systems,
Mokpo National Maritime University,
Mokpo, Jeollanam-do 58628,
South Korea

HIGHLIGHTS

- Hydraulic transients and dynamical analysis have been provided for desalination plants.
- Adaptive sliding mode control is applied for suppression of hydraulic shocks.
- Active controller provides robust performance and stability ensuring water production efficiency and product quality.
- Complete system is implemented with prolonging life expectancy of desalination equipment by sliding mode control.

INTRODUCTION

Generally, water desalination is the process of removing dissolved salts and mineral components from target substances in order to attain quality water for animal consumption, irrigation, and human use. Water management based on desalination technology has become the solution for world water scarcity for many decades. Especially, desalinated water is the main water source for meeting the water demands in water-scarce regions. Most of the modern interests in desalination have focused on developing effective ways of providing fresh water for human consumption in regions where the availability of fresh water is extremely limited. Desalination plants have been designed to consistently

doi: 10.2166/ws.2021.032

produce fresh water from salty feed to system output in sufficient quality as economically as possible. The major technologies utilized for desalination processes include reverse osmosis (RO) and multistage flash distillation (MSF). Recently, the RO has gained more dominance, particularly for brackish water treatments (Alatiqi *et al.* 1999). This desalination technique has also been used in diverse processing industries such as chemical, nuclear, biotechnology, and petroleum (Jamal *et al.* 2004). The fundamental RO principle is based on the transport mechanisms of solvent and solute through semi-permeable membranes for water treatments, using high pressure. Yet, this system is of considerable complexity in terms of its biological and physical aspects. A number of desalination researches have been conducted to realize a variety of water treatment mechanisms in existing technologies. Generally, the RO transport mechanisms can be divided into four main types (Ghernaout 2017): the wetted surface (Reid & Breton 1959), the solution–diffusion (Lonsdale *et al.* 1965), the sieve (Banks & Sharples 1966), and the preferential sorption–capillary flow mechanism (Sourirajan 1986). Consequently, many RO models have been presented in literature, including the models of Senthilmurugan *et al.* (2005), Oh *et al.* (2009), Sundaramoorthy *et al.* (2011), and Chaabene *et al.* (2018). Some transfer functions have been also proposed for RO control purposes such as those of Robertson *et al.* (1996), Alatiqi *et al.* (1999), Riverol & Pilipovik (2005), Bartman *et al.* (2009), and Chaaben *et al.* (2011). A better quantitative understanding in terms of process dynamics is thus required to enhance plant performance. Due to uncertainties and disturbances in the real-time operations, the design of robust monitoring systems of a large RO process is one of the most challenging jobs in water desalination plants. The plant uncertainties can be parametric uncertainty due to modeling mismatch, unmodeled dynamics, and simplification or parameter changes because of disruptions such as concentration polarization, feed concentration, fouling and scaling. The external disturbances are possibly feed-concentration change, leakage or more severe disturbances caused by, for example, hydraulic transients. Therefore, a robust dynamic controller is required to cope with a RO desalination plant confronting these challenges to increase productivity and prolong the life of plant components (Sobana & Panda 2011). RO literature shows that although there are more and more challenges in controlling RO systems, current controllers are mostly proportional-integral-derivative (PID) based (Alatiqi *et al.* 1989; Kim *et al.* 2009; Rathore *et al.* 2013; Chithra *et al.* 2015; Ncube & Inambao 2019; Patnana *et al.* 2020), and model predictive control (MPC) (Abbas 2006; Bartman *et al.* 2009; Sobana & Panda 2014; Rivas-Perez *et al.* 2019; Kargar & Mehrad 2020; Mehrad & Kargar 2020). Furthermore, there are very few studies considering robust control synthesis of desalination plants under parametric uncertainties and disturbances such as water hammering. PID, MPC, and sliding mode control (SMC) algorithms are some of the best for regulating perturbed dynamical systems with uncertainties and disturbances in many industrial applications (Edwards & Spurgeon 1998; Utkin *et al.* 1999). The chattering problem of conventional SMC has been solved by high order SMCs (Adjoudj *et al.* 2011; Benbouzid *et al.* 2014; Patnaik *et al.* 2016). In fact, the super-twisting (STW) algorithm is considered as a second-order SMC. The concept of this algorithm is to generate a continuous control function which ensures the convergence of the sliding surface and its derivative in finite time. The standard STW control algorithm requires knowledge of the disturbance bound which is not easy to be estimated in practice (Boubzizi *et al.* 2018). Despite the robustness and applicability of SMC, there are still very few works reported to regulate RO systems (Vrkalovic *et al.* 2018; Zebbar *et al.* 2019) and none of them account for the effects of hydraulics transients such as water hammer. An important consideration in the safe operation of water treatment plants is the suppression of undesirable hydraulic transients, which are also related to water hammer or pressure surge. In the late 1960s, transient flow analyses using method of characteristics (MOC) and digital computers gained favor over graphical methods. In reality, the desalination plants suffer from more frequent and severe environmental variations such as hydraulic and influent flow shock. Most commonly, hydraulic shock occurs when a column of moving non-compressible liquid is suddenly stopped in line pressure. The excessive pressure surges may cause collapse of pipeline or damage of hydraulic equipment in the water treatment system (Bird *et al.* 2002). Larger pressure waves can certainly cause serious safety problems for desalination plants. In many industrial applications, high-pressure waves can burst pipes, valves, and open joints, flanges, etc., and low pressures can collapse

pipes or suck contaminated water into pipes (Chaudhry 2014; Liu & Simpson 2018). Hydraulic shock loads should be kept within the prescribed limits to protect the system components. Traditional passive devices against pressure pulsations and hydraulic shocks do not fully provide emergency protections against system failure due to pipe collapse or bursting (Schmitt *et al.* 2006). To mitigate severe hydraulic surge effects, the active controller can be utilized to minimize pressure fluctuations. Hydraulic transient and its effects has become a major area of concern for many researchers, but few have been involved in actively controlling water surges of desalination plants (Alidai & Pothof 2016; Phuc *et al.* 2017). The goals are to robustly regulate the product water flow and system pressure to track some setpoints and, especially, to stabilize the water productivity under water shock loads. In this paper, an adaptive STW SMC approach (Shtessel *et al.* 2010) is introduced for the desalination system. This algorithm can adapt control parameters to guarantee the convergence of the sliding surface to zero with unknown uncertainties against hydraulic shocks. The STW SMC strategy is effective for controlling of RO systems in normal conditions. However, in case of hash conditions such as water hammer, the robust stability of the RO system controlled by the fixed-gains of STW SMC may not be achieved. Therefore, adaptable control gains are integrated to guarantee the robust performance of the control scheme. Another advantage of this SMC-based controller is that it is readily applicable for deploying into the RO control hardware. The simulation results show that the active control algorithm provides superior performance and is perfectly fitting to water monitoring systems coping with fluid shocks. Finally, the active controller can effectively monitor all the components of desalination plants, taking automatic compensation actions when hydraulic pressure surges occur, with resulting advantages in terms of effective automation and general plant management.

MATERIALS AND METHODS

Hydraulic transients in desalination plants

Basic components of a desalination system are briefly described considering hydraulic interactions among the system devices. In, the mass and momentum transfer under hydraulic shocks are not well understood for water treatment systems. The disadvantages of an RO system are the difficulties of obtaining rigorous mathematical models of desalination process, which accounts for several operating factors such as feed temperature, concentration polarization, and fouling under hydraulic surge waves. The RO controlled system is developed by Bartman *et al.* (2009), in which the overall mass balance and local energy balances are exploited around the valves and combined with additional terms. The schematic diagram of the RO model is depicted in Figure 1. In this simplified system, feed water enters the system and is pressurized by the high-pressure pump to pass through the membranes to the product water. The feed water from the water line valve is first pushed through the pre-filters which protect the semi-permeable RO membranes from physical and chemical damage. The RO desalination system incorporates a high-pressure pump to create the necessary level of force to counter the osmotic pressure ($\Delta\pi$). The remaining water with a high concentration is rejected through the concentration valve. This concentrated flow is controlled by the concentration valve using valve resistance R_{vc}. The bypass valve is to control the bypass flow by the valve resistance R_{vb}. The product water flow F_p and the system pressure P_s are selected as controlled outputs in this study. The feed stream velocity is kept constant at 10 m/s. The product water and system pressure will change their values according to the opening of the control valves. A lack of proper plumbing in the feed water system with pump operations will result in mechanical damage to the RO membrane. Suitable methods for active control systems must be considered to avoid such severe unacceptable flow situation. During operations of dynamical fluid flow systems, such as the desalination process, the unsteady flow conditions will be inevitably encountered. Transient events in the desalination plants usually occur because of actions at pumps and control valves that are detrimental to vulnerable hydraulic components such as filtration and membranes. When hydraulic transients occur too quickly, they induce a rapid change in flow rate within desalination plants and cause potential pressure surges that could lead to detrimental operating conditions. High-pressure upsurges can lead to desalination system failure and excess leakage, where

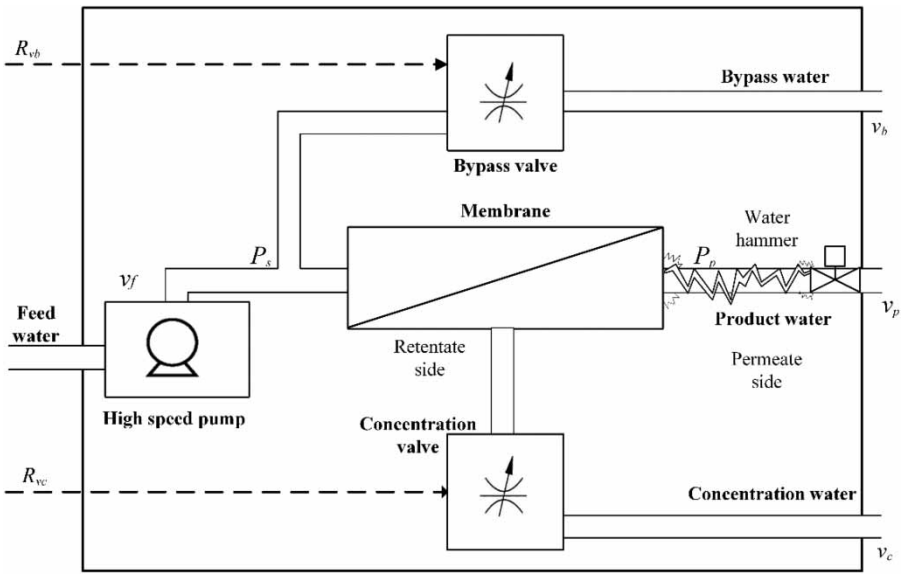

Figure 1 | Schematic diagram of the proposed desalination process.

low-pressure down surges can create vacuum conditions, and system equipment and devices can collapse or burst. What started as a hydraulic surge has now evolved into a vapor condition, itself causing its own bubble collapse hydraulic shock. The primary objectives of transient analysis are to determine the values of transient pressures that can result from flow control operations and to establish the design criteria for system equipment and devices so as to provide a tolerable level of protection. Careful considerations are thus required in the system design stages to make sure that the unsteady fluid operations do not give rise to unacceptable flow and excessive pressure transient conditions.

The model is based on dynamical equations of the flow velocities through the concentration and bypass valve (Bartman *et al.* 2009) and, with some modification at the inputs, is given as follows, respectively:

$$\frac{dv_c}{dt} = \frac{A_p}{V_s}\left(\frac{A_p}{A_m K_m}(v_f - v_c - v_b) + \frac{\Delta\pi}{\rho} - 0.5(R_{v_c} + 120000)v_c^2\right)$$
$$\frac{dv_b}{dt} = \frac{A_p}{V_s}\left(\frac{A_p}{A_m K_m}(v_f - v_c - v_b) + \frac{\Delta\pi}{\rho} - 0.5(R_{v_b} + 120000)v_b^2\right) \quad (1)$$

where V_s is the system volume, A_p the pipe cross-sectional area, A_m the membrane area, K_m the overall mass transfer coefficient of the membrane, ρ the fluid density, R_{vc} and R_{vb} the concentration and bypass valve resistance, respectively, with the working ranges [−120,000, 120,000]; v the water velocity, the subscript f indicates feed stream, b the bypass stream, c the concentration stream, and p the product stream. In Equation (1), $\Delta\pi$ is the osmotic pressure that has to be overcome in order to produce permeate. The valve resistance is a dimensionless quantity which is equal to zero for an absence of resistance and goes to infinity as the valve becomes completely closed. The osmotic pressure difference is a measure of the chemical potential difference between the solution on the feed and permeate side of the membrane. An alternative definition of the osmotic pressure of a solution of concentration at a given temperature is described as follows (Bartman *et al.* 2009):

$$\Delta\pi = C_f \beta T\left(\alpha + (1-\alpha)\left(\frac{(1-R) + R(v_f - v_b)}{v_c}\right)\right) \quad (2)$$

where β indicates the effective concentration to osmotic pressure constant, α the effective concentration weighting coefficient, R the fractional salt rejection of the membrane, and T the temperature. The product water flow F_p and the system pressure P_s can be calculated based on system

variables v_c and v_b using the following equations:

$$F_p = A_p(v_f - v_c - v_b)$$
$$P_s = \frac{A_p\rho}{A_m K_m}(v_f - v_c - v_b) + \Delta\pi = P_p + \Delta\pi \quad (3)$$

where P_p is the permeate pressure. In the area where the velocity change occurs, the liquid pressure increases dramatically due to the momentum force. Transient pressures are most important when the rate of flow is changed rapidly, such as resulting from rapid valve closures or pump stoppages. An excessive pressure rise can cause the membranes and/or materials of construction to move and sometimes break, eventually resulting in a complete failure of the membranes.

Dynamical analysis

A hydraulic shock typically occurs in pipes after a valve is shut off suddenly. Specifically, the quick starting or stopping of pumps can create damaging pressure spikes in the valves known as water hammer. Since liquids are incompressible, when there is a sudden change in fluid velocity, the kinetic energy of the moving fluid is immediately converted into potential energy, causing waves of pressure and flow velocity back to the fluid source. A flow velocity greater than 1.5 m/s, a valve closing in less than 1.5 s, and a high operating pressure will cause, water hammer to occur and the transient pressure can be as high as five times the initial working pressure. Therefore, water hammer phenomenon in RO systems must be sufficiently considered for RO plant design and to avoid plant damages or failure.

The governing equations of water hammer include two partial differential equations (PDEs) and are given as follows (Juneseok 2008; Chaudhry 2014):

$$\frac{\partial Q_d}{\partial t} + gA_p\frac{\partial H}{\partial x} + \frac{f}{2D}Q_d|Q_d| = 0$$
$$\frac{\partial H}{\partial x} + \frac{a^2}{gA_p}\frac{\partial Q_d}{\partial x} = 0 \quad (4)$$

where x is the pipe's length, $Q_d = A_p V$ the discharge flow, $H = P/\rho g$ the piezometric head, f the friction factor, D the pipe internal diameter, and g the gravitational acceleration. a is the wave speed and is calculated by:

$$a = \sqrt{\frac{K_f}{\rho\left(1 + c\frac{K_f D}{eE}\right)}} \quad (5)$$

where K_f is the bulk modulus of fluid elasticity, ρ the density of the liquid, e the pipe thickness, E the Young's modulus of pipe elasticity, and $c = 1 - \nu/2$, in which ν is the Poisson's ratio. Suppose that the studied RO system is working at the steady-state while a sudden closure occurs at the permeate side that is 20 m away from the membrane – the steady-state value of permeate side pressure P_{pss} is 22.97 bar and those of velocities through the permeate, concentration, and bypass valve are 5 m/s, 1 m/s, and 4 m/s, respectively. All the components are supposed to be in the same horizontal plane. Since the governing equations are nonlinear PDEs, the numerical method of McCormack (McCormack & Baldwin 1975) is used for solving these equations to simulate the transient pressure and velocity of the water flow in RO systems during a water hammer. The profile of the pressure waves at the permeate valve and the profile of the velocity wave at the membrane side are illustrated in Figure 2.

It can be observed that the magnitude of the first pressure wave is the peak. Specifically, the maximum pressure $P_{p\max}$ is 82.57 bar, which is approximately 3.6 times as big as the steady-state one. The first velocity wave only equals the initial flow velocity through the permeate valve. The simulation result agrees with the famous Joukowski pressure change of (Joukowski 1904) to calculate the maximum pressure in the water hammer. It is worth noting that in general, the RO membrane can stand a maximum pressure surge of about 80 bar. Hence this hammer transient pressure will cause rupture or damage to the pump, valves, piping, or fittings. Furthermore, the water hammer will create vapor cavitation and column separation during its pressure waves in the vacuum which are lower than 0.03 bar of the vapor pressure with water temperature at 25 °C. These phenomena will be very harmful to the desalination system by increasing the potential for cavitation erosion and resonance of water column collision as well as two-phase flow instability within the pipes. The hammer wave profiles in Figure 2 are

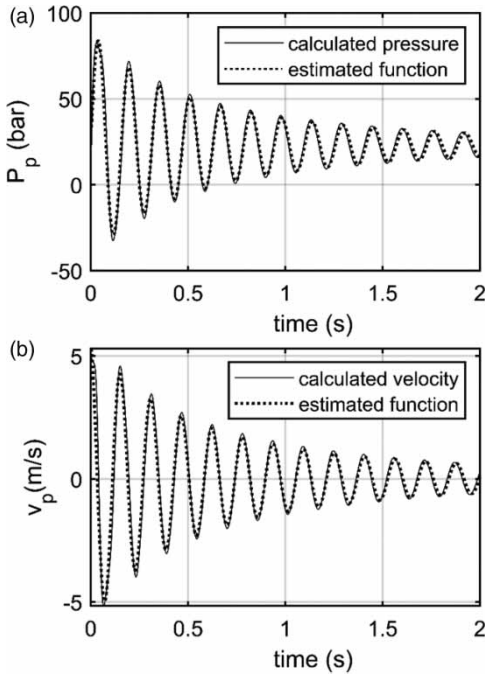

Figure 2 | Water hammer wave profiles: (a) transient pressure and (b) concentration flow velocity.

simulated by McCormack's numerical method. In order to incorporate the water hammering as disturbance into the mathematical model, the pressure and velocity profiles are approximated by the following function, respectively:

$$P_p = A_{pp}\sin(\omega_h t) + P_{pss}$$
$$V_p = A_v \sin(\omega_h t + \varphi_{vh}) \tag{6}$$

where:

$$A_{pp} = \frac{A_{pg}}{(t+0.95)^2}, A_{pg} = P_{p\max} - P_{hss} = 59.6,$$
$$\omega_h = 1/0.025, P_{pss} = 22.97 \tag{7}$$
$$A_{pv} = \frac{V_{pss}}{(t+0.93)^2}, V_{pss} = 5, \varphi_{vh} = 1.8$$

The comparison of the approximated functions and the numerical hammer wave profiles are also illustrated in Figure 2, which shows good fitting between them. The water hammer in the permeate side will affect the whole system including system pressure and velocities through the concentration and bypass valve. From the dynamic equation of the RO system, the system flow velocities can be calculated easily. As plotted in Figure 3, their profiles are also approximated as follows:

$$v_c = \frac{13}{(t+1)^2}\sin(\omega_h t - 0.145) + 5.9$$
$$v_b = \frac{27}{(t+1)^2}\sin(\omega_h t + 0.12) + 4.1 \tag{8}$$

From Figure 3, it can be seen that the directions of the flows through the valves are alternately inverted, causing strong disturbances to the dynamic behaviors of the RO system. With no surge protection, transient wave profiles are unacceptably high, and if the reduced pressure is below the vapor pressure, a steam bubble will form (a large cavitation). It is noted that fluid fluctuation effects may disturb overall operations of the hydraulic system. This potentially dangerous (or undesirable) phenomenon can be mitigated with suitable design practice or active process controller. The oscillation functions in Equation (8) will be incorporated into the numerical simulation as external disturbances to check the system performance. Transient behaviors were be eliminated and maximum pressures were reduced until they

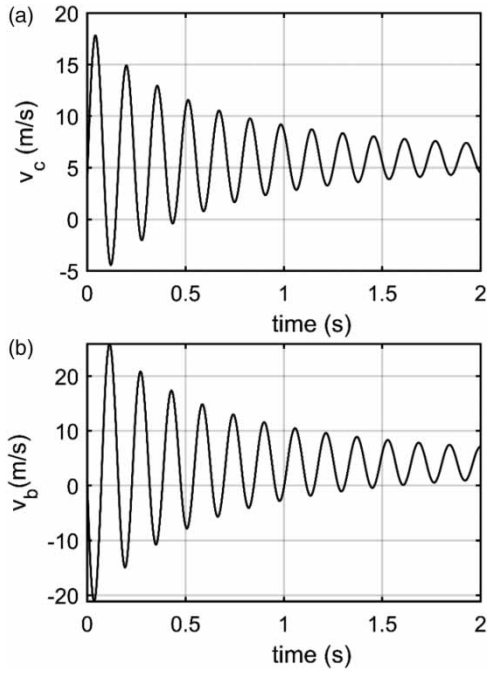

Figure 3 | Velocity wave profiles of v_c and v_b under water hammer.

coincided with steady-state pressures. The identification and calculation of pressures, velocities, and other abnormal behaviors resulting from hydraulic transients make possible the effective use of various control strategies in order to minimize energy and fluid losses or to improve the system capacity and the water quality.

Adaptive SMC synthesis

Since operating valves and pumps could suddenly cause severe hydraulic transient effects, the active controller $u(t)$ must be manipulated carefully to minimize wave fluctuations. By allowing the state variables $x_1 = v_c$ and $x_2 = v_b$, the nonlinear RO model in Equation (1) is rewritten in state-space form as follows:

$$\begin{aligned}\dot{x}_1 &= A_{RO1}(v_f - x_1 - x_2) + A_{RO2}\Delta\pi - 0.5(u_2 + 120000)A_{RO3}x_1^2\\ \dot{x}_2 &= A_{RO1}(v_f - x_1 - x_2) + A_{RO2}\Delta\pi - 0.5(u_2 + 120000)A_{RO3}x_2^2\end{aligned} \tag{9}$$

where:

$$\Delta\pi = C_f\beta T\left(\alpha + (1-\alpha)\left(\frac{(1-R) + R(v_f - x_2)}{x_1}\right)\right) \tag{10}$$

$$A_{RO1} = \frac{A_p^2}{A_m K_m V_s}, A_{RO2} = \frac{A_p}{\rho V_s}, A_{RO3} = \frac{A_p}{V_s} \tag{11}$$

The state-space representation in Equation (9) can be formulated in the compact form as follows:

$$\dot{x} = f(x,t) + b(x,t)u \tag{12}$$

where the state vector and nonlinear terms are given by:

$$\dot{x} = \begin{bmatrix}\dot{x}_1\\ \dot{x}_2\end{bmatrix},\ b(x,t) = \begin{bmatrix}-0.5A_{RO3}x_1^2 & 0\\ 0 & -0.5A_{RO3}x_2^2\end{bmatrix} \tag{13}$$

$$f(x,t) = \begin{bmatrix}A_{RO1}(v_f - x_1 - x_2) + A_{RO2}\Delta\pi - 60000A_{RO3}x_1^2\\ A_{RO1}(v_f - x_1 - x_2) + A_{RO2}\Delta\pi - 60000A_{RO3}x_2^2\end{bmatrix} \tag{14}$$

The sliding variables are selected as follows:

$$s_1 = x_1 - x_{1ref},\ s_2 = x_2 - x_{2ref} \tag{15}$$

Then the state-space representation of the sliding mode variables can be written as:

$$\begin{bmatrix}\dot{s}_1\\ \dot{s}_2\end{bmatrix} = \begin{bmatrix}A_1\\ A_2\end{bmatrix} + \begin{bmatrix}B_{11} & 0\\ 0 & B_{22}\end{bmatrix}\begin{bmatrix}u_1\\ u_2\end{bmatrix} \tag{16}$$

where:

$$\begin{aligned}A_1 &= A_{RO1}(v_f - x_1 - x_2) + A_{RO2}\Delta\pi - 60000A_{RO3}x_1^2 - \dot{x}_{1ref}\\ &\triangleq A_{10} + \delta A_1\\ A_2 &= A_{RO1}(v_f - x_1 - x_2) + A_{RO2}\Delta\pi - 60000A_{RO3}x_2^2 - \dot{x}_{2ref}\\ &\triangleq A_{20} + \delta A_2\end{aligned} \tag{17}$$

$$\begin{aligned}B_{11} &= -0.5A_{RO3}x_1^2 \triangleq B_{110} + \delta B_{11}\\ B_{22} &= -0.5A_{RO3}x_{12}^2 \triangleq B_{220} + \delta B_{22}\end{aligned} \tag{18}$$

where A_1, A_2, B_{110}, and B_{220} are the known nominal parts, while δA_1, δA_2, δB_{11}, and δB_{22} describe the perturbed parts representing all model uncertainties.

Then, the control problem is equivalent to the finite-time stabilization of the following system:

$$\begin{bmatrix}\dot{s}_1\\ \dot{s}_2\end{bmatrix} = A + B\begin{bmatrix}u_1\\ u_2\end{bmatrix} \tag{19}$$

where:

$$\begin{aligned}A &= \begin{bmatrix}A_{10}\\ A_{20}\end{bmatrix} + \begin{bmatrix}\delta A_1\\ \delta A_2\end{bmatrix} \triangleq A_0 + \delta A\\ B &= \begin{bmatrix}B_{110} & 0\\ 0 & B_{220}\end{bmatrix} + \begin{bmatrix}\delta B_{11} & 0\\ 0 & \delta B_{22}\end{bmatrix} \triangleq B_0 + \delta B\end{aligned} \tag{20}$$

In order to drive the sliding variables to converge to zero and to achieve an input–output feedback linearization, the controller is realized as follows:

$$u = B_0^{-1}[-A_0 + w] = -B_0^{-1}A_0 + B_0^{-1}w \tag{21}$$

where the former term is the equivalent control part and the latter is the reaching part. By considering external disturbance and uncertainty, Equation (19) can be written as

follows:

$$\dot{s} = A + Bu = A_0 + \delta A + (B_0 + \delta B)[B_0^{-1}(-A_0 + w)] \tag{22}$$

Or it can be rewritten in the following form:

$$\begin{bmatrix} \dot{s}_1 \\ \dot{s}_2 \end{bmatrix} = \begin{bmatrix} \hat{A}_1 \\ \hat{A}_2 \end{bmatrix} + \begin{bmatrix} \hat{B}_{11} & 0 \\ 0 & \hat{B}_{22} \end{bmatrix} \begin{bmatrix} w_1 \\ w_2 \end{bmatrix} \tag{23}$$

where:

$$\begin{aligned} &\hat{A}_1 = \delta A_1 - \frac{\delta B_{11}}{B_{110}} A_{10}, \hat{A}_2 = \delta A_2 - \frac{\delta B_{22}}{B_{220}} A_{10} \\ &\hat{B}_{11} = 1 + \frac{\delta B_{11}}{B_{110}}, \hat{B}_{22} = 1 + \frac{\delta B_{22}}{B_{220}}, w = \begin{bmatrix} w_1 \\ w_2 \end{bmatrix} \end{aligned} \tag{24}$$

In the reaching part of the controller, the action w is designed to deal with disturbances and uncertainties to guarantee the reachability of the sliding surfaces in Equation (15). The control synthesis of w is based on the approach proposed by Shtessel *et al.* (2010), where the following theorem provides sufficient condition to guarantee the stability and robustness of the RO system. Again, the external disturbances such as hydraulic transients can create serious consequences for water utilities if not properly recognized and addressed by proper analysis.

Theorem 1: Consider the RO system in Equation (9) and the sliding surface in Equation (15). The controlled RO system is guaranteed to provide its robustness to uncertainties and finite-time convergence if the adaptive STW SMC law is designed as follows:

$$\begin{aligned} &w_1 = -\alpha_1 |s_1|^{1/2} \mathrm{sgn}(s_1) + v_1 \\ &\dot{v}_1 = -\beta_1 \mathrm{sgn}(s_1) \\ &w_2 = -\alpha_s |s_2|^{1/2} \mathrm{sgn}(s_2) + v_2 \\ &\dot{v}_2 = -\beta_2 \mathrm{sgn}(s_2) \end{aligned} \tag{25}$$

Here, the control gains α and β are updated as follows:

$$\begin{aligned} &\alpha_{i(i=1,2)} = \begin{cases} \omega_i \sqrt{\frac{\gamma_i}{2}}, & \text{if} |s_i| > \psi_i \\ 0, & \text{if} |s_i| \le \psi_i \end{cases} \\ &\beta_{i(i=1,2)} = 2\varepsilon_i \alpha_i + \lambda_i + 4\varepsilon_i \end{aligned} \tag{26}$$

where ω_i, γ_i, ψ_i, λ_i, and ε_i are arbitrary positive constants ($\in \Re^+$).

Proof: For the state variable x_1, its corresponding sliding surface from Equation (23) is given by:

$$\dot{s}_1 = \hat{A}_1 + \hat{B}_{11} w_1 \tag{27}$$

Assume that $\hat{A}_1$ is a bounded function which satisfies the following condition:

$$|\hat{A}_1| < \delta_1 |s_1|^{1/2} \tag{28}$$

where δ_1 is a positive constant ($\in \Re^+$). From Equations (25) and (27), the first sliding variable (s_1) can be expressed as:

$$\begin{aligned} &\dot{s}_1 = -\alpha_1 \hat{B}_{11} |s_1|^{1/2} \mathrm{sgn}(s_1) + v_1 + \hat{A}_1 \\ &\dot{v}_1 = -\beta_1 \hat{B}_{11} \mathrm{sgn}(s_1) \end{aligned} \tag{29}$$

A new vector z is introduced as:

$$z = (z_1, z_2)^T = (|s_1|^{1/2} \mathrm{sgn}(s_1), v_1)^T \tag{30}$$

Its time derivative can be calculated as follows:

$$\begin{aligned} &\dot{z}_1 = \frac{1}{z_1} \left(-\frac{\alpha_1 \hat{B}_{11}}{2} z_1 + \frac{1}{2} z_2 + \frac{1}{2} \hat{A}_1 \right) \\ &\dot{z}_2 = -\frac{\beta_1 \hat{B}_{11}}{|z_1|} z_1 \end{aligned} \tag{31}$$

Exploiting the assumption in Equation (28), the following expression is obtained:

$$\hat{A}_1 = \rho_1(x, t) |s_1|^{1/2} \mathrm{sgn}(s_1) = \rho_1(x, t) z_1 \tag{32}$$

where $\rho_1(x, t)$ is a bounded function such as:

$$0 < \rho_1(x, t) < \delta_1 \tag{33}$$

Then Equation (31) can be written as:

$$\dot{z} = A(z_1, z_2) z \tag{34}$$

where:

$$A(z_1, z_2) = \frac{1}{2|z_1|}\begin{bmatrix} -\alpha_1\hat{B}_{11} + \rho_1 & 1 \\ -\beta_1\hat{B}_{11} & 0 \end{bmatrix} \tag{35}$$

The following Lyapunov function candidate (Boubzizi *et al.* 2018) can be used to prove the stability of Equation (34):

$$V(z_1, z_2, \beta_1)^T = V_0 + \frac{1}{2\gamma_1}(\alpha_1 - \bar{\alpha}_1)^2 + \frac{1}{2\gamma_{11}}(\beta_1 - \bar{\beta}_1)^2 \tag{36}$$

Here, V_0 is given by:

$$V_0 = (\lambda_1 + 4\varepsilon_1^2)z_1^2 + z_2^2 - 4\varepsilon z_1 z_2 = z^T P z \tag{37}$$

where P is a positive define matrix:

$$P = \begin{bmatrix} \lambda_1 + 4\varepsilon_1^2 & -2\varepsilon_1 \\ -2\varepsilon_1 & 1 \end{bmatrix} \tag{38}$$

with $\lambda_1 > 0$, $\gamma_{11} > 0$, $|\alpha_1| < \bar{\alpha}_1$, and $|\beta_1| < \bar{\beta}_1$, $\quad \forall t > 0$.

Then the time derivative of the Lyapunov function is:

$$\dot{V}(z, \alpha, \beta)^T = z^T[A^T P + PA]z + \frac{1}{\gamma_1}\varepsilon_{\alpha 1}\dot{\alpha}_1 + \frac{1}{\gamma_{11}}\varepsilon_{\beta 1}\dot{\beta}_1 \tag{39}$$

where $\varepsilon_{\alpha 1} = (\alpha_1 - \bar{\alpha}_1)$, and $\varepsilon_{\beta 1} = (\beta_1 - \bar{\beta}_1)$. Note that:

$$z^T[A^T P + PA]z = \dot{V}_0(z_1, \alpha_1, \beta_1)^T \le -\frac{1}{2|z_1|}z^T Q z \tag{40}$$

where:

$$Q = \begin{bmatrix} Q_{11} & Q_{12} \\ Q_{21} & 4\varepsilon_1 \end{bmatrix} \tag{41}$$

with:

$$\begin{aligned} Q_{11} &= 2\lambda_1\alpha_1\hat{B}_{11} + 4\hat{B}_{11}\varepsilon_1(2\varepsilon_1\alpha_1 - \beta_1) - 2\rho_1(\lambda_1 + 4\varepsilon_1^2) \\ Q_{12} &= Q_{21} = (\beta_1\hat{B}_{11} - 2\varepsilon_1\alpha_1\hat{B}_{11} - \lambda_1 - 4\varepsilon_1^2) + 2\varepsilon_1\rho_1 \end{aligned} \tag{42}$$

By selecting $\beta_1 = 2\varepsilon_1\alpha_1 + \lambda_1 + \varepsilon_1^2$, the matrix Q is positive definite if α_1 satisfies the following inequality:

$$\alpha_1 > \frac{\delta_1(\lambda_1 + 4\varepsilon_1^2) + 2\varepsilon_1(\lambda_1 + \varepsilon_1^2)}{\lambda_1\hat{B}_{11}} \tag{43}$$

From Equation (40), it is bounded by:

$$\dot{V}_0(z) \le -\frac{1}{2|z_1|}z^T Q z \le \frac{2\varepsilon_1}{2|z_1|}z^T z = \frac{\varepsilon_1}{|z_1|}\|z\|^2 \tag{44}$$

By allowing $\lambda_{\min}(P)$ and $\lambda_{\max}(P)$ as the minimum and maximum eigenvalues, it is known that:

$$\lambda_{\min}(P)\,\|z\|^2 \le z^T P z \le \lambda_{\max}(P)\|z\|^2 \tag{45}$$

Equation (32) can be rewritten as:

$$\|z\|^2 = z_1^2 + z_2^2 = |s_1| + z_2^2 \tag{46}$$

and

$$|z_1| = |s_1|^{1/2} \le \|z\| \le \frac{V_0^{1/2}(z)}{\lambda_{\min}^{1/2}(P)} \tag{47}$$

Then it can be concluded that:

$$\dot{V}_0(z) \le -rV_0^{1/2} \tag{48}$$

where:

$$r = \frac{\varepsilon_1\lambda_{\min}^{1/2}(P)}{\lambda_{\max}(P)} \tag{49}$$

Combining Equations (36) and (48), then it follows that:

$$\begin{aligned} \dot{V} \le -rV_0^{1/2} - \frac{k_1}{\sqrt{2\gamma_1}}|\varepsilon_{\alpha 1}||s_1| - \frac{k_{11}}{\sqrt{2\gamma_{11}}}|\varepsilon_{\beta 1}||s_1| + \frac{1}{\gamma_1}\varepsilon_{\alpha 1}\dot{\alpha}_1 + \\ \frac{1}{\gamma_{11}}\varepsilon_{\beta 1}\dot{\beta}_1 + \frac{k_1}{\sqrt{2\gamma_1}}|\varepsilon_{\alpha 1}||s_1| + \frac{k_{11}}{\sqrt{2\gamma_{11}}}|\varepsilon_{\beta 1}||s_1| \end{aligned} \tag{50}$$

It is well known that:

$$(x^2+y^2+z^2)^{1/2} \le |x|+|y|+|z| \tag{51}$$

From Equation (50) it can be derived as:

$$\begin{aligned} &-rV_0^{1/2} - \frac{k_1}{\sqrt{2\gamma_1}}|\varepsilon_{\alpha 1}||s_1| - \frac{k_{11}}{\sqrt{2\gamma_{11}}}|\varepsilon_{\beta 1}||s_1| \\ &\le -\eta_1\left[V_0 + \frac{1}{2\gamma_1}(\varepsilon_{\alpha 1}s_1)^2 + \frac{1}{2\gamma_{11}}(\varepsilon_{\beta 1}s_1)^2\right]^{1/2} \end{aligned} \tag{52}$$

where $\eta_1 = \min(r, k_1, k_{11})$. By allowing $V_1 = V_0 + \frac{1}{2\gamma_1}(\varepsilon_{\alpha 1}s_1)^2 + \frac{1}{2\gamma_{11}}(\varepsilon_{\beta 1}s_1)^2$, then it can be further described as:

$$\begin{aligned} \dot{V}(z,\alpha_1,\beta_1) &\le -\eta_1 V_1^{1/2} - |\varepsilon_{\alpha 1}|\left[\frac{1}{\gamma_1}\dot{\alpha}_1 - \frac{k_1}{\sqrt{2\gamma_1}}|s_1|\right] \\ &- |\varepsilon_{\beta 1}|\left[\frac{1}{\gamma_{11}}\dot{\beta}_1 - \frac{k_{11}}{\sqrt{2\gamma_{11}}}|s_1|\right]\frac{k_1}{\sqrt{2\gamma_1}}|\varepsilon_{\alpha 1}||s_1| \\ &- \frac{k_{11}}{\sqrt{2\gamma_{11}}}|\varepsilon_{\beta 1}||s_1|\left[V_0 + \frac{1}{2\gamma_1}(\varepsilon_{\alpha 1}s_1)^2 + \frac{1}{2\gamma_{11}}(\varepsilon_{\beta 1}s_1)^2\right] \\ &= -\eta_1 V_1^{1/2} + \xi \end{aligned} \tag{53}$$

By choosing $\xi = 0$, the finite-time convergence can be assured via the following adaptive gains:

$$\begin{aligned} \dot{\alpha}_1 &= k_1\sqrt{\frac{\gamma_1}{2}}|s_1| \\ \beta_1 &= 2\varepsilon_1\alpha_1 + \lambda_1 + 4\varepsilon_1^2 \\ \dot{\beta}_1 &= 2\varepsilon_1\dot{\alpha}_1 = k_{11}\sqrt{\frac{\gamma_{11}}{2}}|s_1| \end{aligned} \tag{54}$$

By selecting $\varepsilon_1 = k_{11}\sqrt{\frac{\gamma_{11}}{2}}|s_1|$, then $\xi = 0$ can be guaranteed. Therefore, the derivative of the given Lyapunov function is ensured to be negative definite, and thus the convergence of $s_1 = 0$ can be written as:

$$\dot{V}(z,\alpha_1,\beta_1) \le -\eta_1 V_1^{1/2}, \text{ with } \eta_1 > 0 \tag{55}$$

The proof is completed for the state variable x_1. Similarly, the same justification can be made to prove the stability of the state variable x_2. The adaption laws for control gains utilize the current information on the sliding surface to adjust the control input in real time.

RESULTS AND DISCUSSION

Transient events are also significant for water quality as well as productivity in the desalination plants. Hydraulic shocks in particular can cause damages or fracture to the related components of desalination plants. Thus, the hydraulic transient studies with water hammering should be included in the design stage for RO plants. The numerical simulation is carried out at working steady-state ($v_r = 4$, $v_b = 1$, and $v_p = 5$). The current product flow rate and the system pressure are 2,286 L/h and 35.69 bar, respectively. The set-points are 2,000 L/h and 40 bar, respectively. Since closing the valve suddenly could cause severe hydraulic shock effects, the active controller $u(t)$ must be manipulated carefully to minimize flow fluctuations. The adaptive STW SMC controller has been successfully designed for the RO desalination system with the selected control parameters as follows: $\varepsilon_{1,2} = 1$, $\gamma_{1,2} = 1$, $\lambda_{1,2} = 1$, $\omega_1 = 6$, and $\omega_2 = 8.5$. The proposed SMC scheme with adaption is intended to minimize the control activities along with a finite-time convergence against water hammer. Figure 4 shows the step responses of the controlled variables. It can be seen that the product flow rate F_p and the system pressure P_s can reach new set-points with settling time within approximately 1 s, which is better than the other results reported in RO literature as summarized in Table 1. It is worth noting that previous studies do not provide clarity on water hammer. As depicted in Figure 4, there is a slight overshoot in the flow rate and no overshoot in the pressure channel. The fast responses demonstrate that the active controller can quickly drive the system to desired steady-states under some variations.

Figure 5 shows the tracking errors and the finite-time convergence to the sliding surfaces. It is noted that the set-point tracking in the RO plant is guaranteed to converge to zero with in a time limit of approximately 1 s. When the system states reach the sliding surfaces, they will converge to the set-points and be kept there until new desired values are set.

One of important issues in the SMC algorithm is the control actions. The classic SMC uses a discontinuous

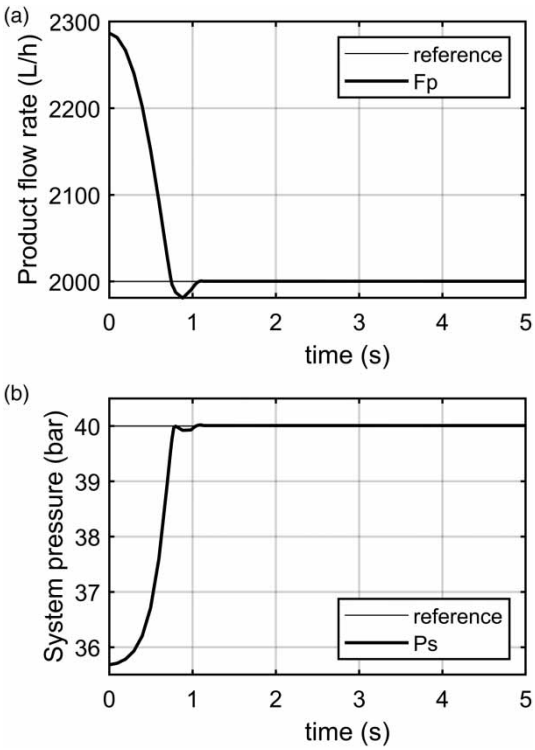

Figure 4 | Transient responses of the controlled desalination system.

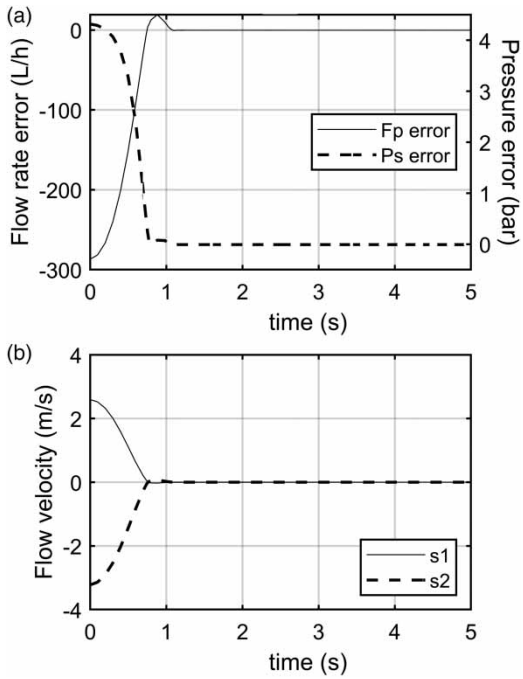

Figure 5 | Tracking errors and sliding variable convergences.

Table 1 | Comparison of control strategies performance

Control algorithm	PID (Gambier 2011)	MPC	SMC (Vrkalovic et al. 2018)	STW SMC (Zebbar et al. 2019)	Proposed Adaptive STW SMC
Set-point (L/h)	35	350	227	NA	2,000
Settling time (s)	1.5	4	1.5	1.5	1

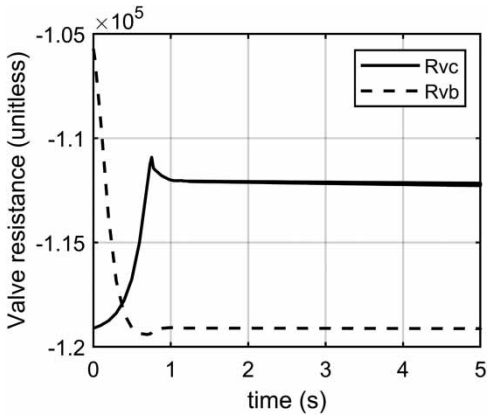

Figure 6 | Control activity signals for set-point tracking.

control action. If the control action is discontinuous in the state variables, it causes chattering problem which is undesirable in the practical implementations. In this work, the control signals are plotted in Figure 6 by implementing smooth control input. It can be observed that there is almost no chattering and the signals are not saturated due to the characteristics of the STW algorithm. This control scheme also guarantees the fast convergence of the sliding surfaces as illustrated in Figure 5. It helps protect against machine damages and prolongs the lifespan of the operating valves.

For the control synthesis, the most interesting concern is the ability of disturbance attenuation, especially large disturbances such as water hammer, and more generally, fluid hammer. It is noted that this fluid hammer in liquid line can develop peak pressures several times greater than normal working pressures. In this simulation, the water hammer occurring at the permeate side is considered as a disturbance to the RO system. There are always pressure-reducing valves (PRV) installed in RO systems but they are not enough to eliminate hydraulic shock effects. As

discussed earlier, the hammer transient pressure has a damping wave profile and the magnitude of the first peak pressure wave is extremely high. Vacuum pressure also occurs, and both phenomena is very harmful to the RO system. Therefore, not only high positive pressure waves but also negative ones must be regulated to avoid machine or component fatigue failures. The advanced controllers can effectively handle this kind of sporadic disturbance to protect the desalination plants from damages or successfully eliminate erratic sounds coming out.

In this paper, the adaptive STW SMC is proposed to minimize the effect of this water hammer. The initial permeate pressure is 22.97 bar. The simulated condition is chosen as the worst case with the feed water concentration $C_f =$ 50,000 mg/L. As illustrated in Figure 7, the peak pressure in the first wave is calculated at 82.57 bar without the controller. By realizing the proposed controller, this peak pressure is reduced to 24.3 bar, in which the disturbance has been significantly rejected by active controller, or eliminated to approximately 97%. This result demonstrates superior performance compared to 33.33%, which is the best result reported in the literature, where water hammering is attenuated by a PRV; or 58% disturbance attenuation as reported by Phuc *et al.* (2017). It is also noted that the controller prevents air being sucked into the RO system while avoiding every possible vacuum. As a result, the membrane is safely protected, and no vapor cavitation and column separation occur. The ability to deal with this high disturbance proves that the proposed controller can cope with slight perturbation such as fouling or scaling. Although the proposed controller has the ability to diminish the effect of water hammer, a surge tank should always be installed at a suitable location in RO systems for ultimate safety (Liu & Simpson 2018; Shi *et al.* 2019; Zhang *et al.* 2019).

Referring to Figure 7, even though the transient pressure has the sinusoidal wave profile with positive and negative values, the RO system is regulated effectively by the active controller. As illustrated in Figure 8, the control signals produced by the proposed controller provide the reduced chattering without saturation. In fact, the chattering is the main obstacle for its implementation. This control action is done automatically by changing the valves opening in a manner appropriating for the values of the transient pressure. The greatly reduced pressures are realized when surge protection is provided by an active control system. Transient behaviors have been immediately reduced until they coincided with steady-state values.

As mentioned earlier, the control parameters are adaptable so that the controller is more flexible to deal with uncertainties and disturbances. Figure 9 shows that the control gains are updating their values during water hammering. It can be observed that their values increase rapidly when the water hammer has just occurred. When the pressure is dramatically dampened, these values will be fixed or constant. An adaption scheme is developed to update the controller gains providing superior responses, eventually resulting in minimization of chattering effects under hydraulic shock waves. This study presents the basic concepts associated with transient flow, discusses the hydraulic surges, and introduces features of RO system design that

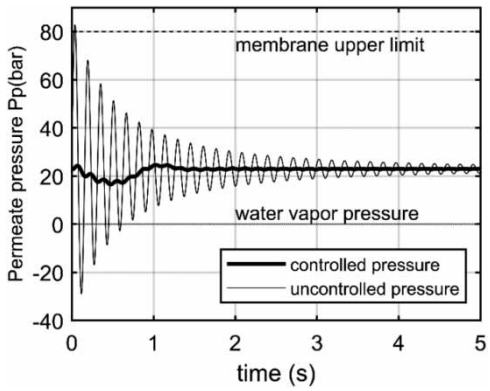

Figure 7 | Controlled transient pressure under water hammer.

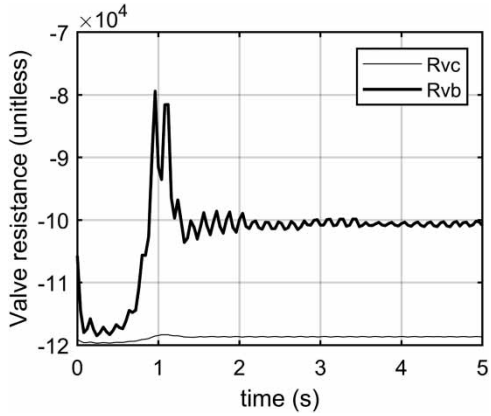

Figure 8 | Control signals under water hammer.

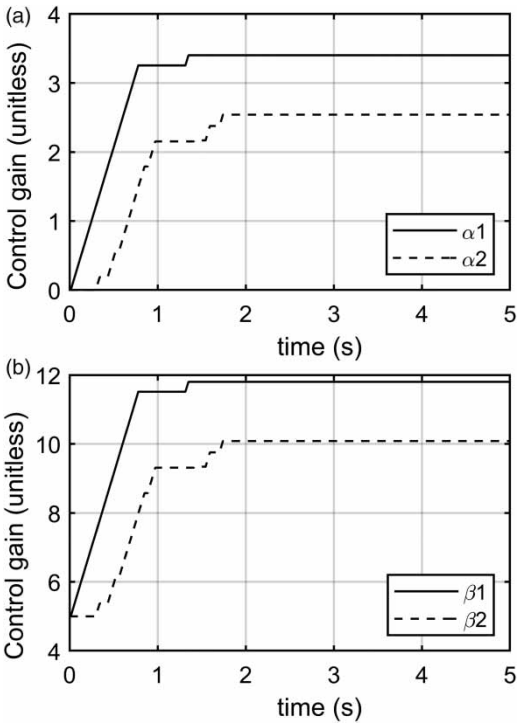

Figure 9 | Adaptive parameters for control gains under water hammer.

should be considered during transient behaviors. The active controllers can eliminate hydraulic transients to protect the desalination plants while enhancing overall performance and reliability of system components in the water treatment applications.

CONCLUSIONS

Hydraulic shocks can have detrimental effects on pipes, pumps, membranes, and valves in the water desalination plants. This paper deals with comprehensive dynamical analysis and control synthesis for hydraulic transients of desalination plants. The robust monitoring of the water desalination plant is challenged by uncertainties and disturbances such as fouling, scaling, and environment changes. First, the dynamic analysis was conducted to investigate the system parameters that affect the water hammer effects. Next, a robust control system was proposed based on SMC scheme with adaptive law. The STW algorithm was implemented to alleviate chattering caused by discontinuous control structure, and to ensure robust performances of the controller in transient states. After realizing adaptive STW SMC algorithm for desalination plants, numerical simulations were carried out in order to validate the effectiveness of the proposed control scheme. The proposed control strategy provides the following novel features to the desalination system:

- The robust control synthesis exploits the adaptive STW SMC strategy to provide the finite-time convergence of the sliding surface while maintaining robust performance and stability against uncertainties and disturbances.
- The proposed controller ensures the tracking of product water flow and pressure set-points in a short time.
- Transient pressure waves can be suppressed to prevent damages or fractures caused by excess pressure or vapor cavitation.
- The presented approach provides a chattering-free SMC synthesis for the hydraulic shocks.

The presented active controllers can eliminate hydraulic shocks to protect the desalination system while enhancing overall performance and reliability. Finally, the validity and the superiority of the water production performances of the adaptive STW SMC scheme over other control algorithms have been clearly demonstrated through numerical simulations as safe and reliable to use in a desalination process.

DATA AVAILABILITY STATEMENT

All relevant data are included in the paper or its Supplementary Information.

REFERENCES

Abbas, A. 2006 Model predictive control of a reverse osmosis desalination unit. *Desalination* **194**, 268–280.

Adjoudj, M., Abid, M., Aissaoui, A., Ramdani, Y. & Bounoua, H. 2011 Sliding mode control of doubly fed induction generator for wind energy turbine. *Revue Roumaine des Sciences Techniques - Serie Électrotechnique et Énergétique* **56**, 15–24.

Alatiqi, I., Ghabris, A. & Ebrahim, S. 1989 System identification and control of reverse osmosis desalination. *Desalination* **75**, 119–140.

Alatiqi, I., Ettouney, H. & El-Dessouky, H. 1999 Process control in water desalination industry: overview. *Desalination* **126**, 15–32. doi: 10.1016/S0011-9164(99)00151-4.

Alidai, A. & Pothof, I. W. M. 2016 Guidelines for hydraulic analysis of treatment plants equipped with ultrafiltration and reverse osmosis membranes. *Desalination and Water Treatment* **57** (5), 1917–1926.

Banks, W. & Sharples, A. 1966 Studies on desalination by reverse osmosis: III. Mechanism of solute rejection. *Journal of Applied Chemistry* **16**, 153–158.

Bartman, A. R., McFall, C. W., Chritofides, P. D. & Cohen, Y. 2009 Model-predictive control of feed flow reversal in a reverse osmosis desalination process. *Journal of Process Control* **19**, 433–442.

Benbouzid, M., Beltran, B., Amirat, Y., Yao, G. & Han, J. 2014 Second-order sliding mode control for DFIG based wind turbines fault ride-through capability enhancement. *ISA Transactions* **53**, 827–833.

Bird, R. B., Stewart, W. E. & Lightfoot, E. N. 2002 *Transport Phenomena*, 2nd edn. John Wiley and Sons, New York.

Boubzizi, S., Abid, H., Hajjaji, A. E. & Chaabane, M. 2018 Adaptive super-twisting sliding mode control for wind energy conversion system. *IJAER* **13** (6), 3524–3532.

Chaaben, A. B., Andoulsi, R., Sellami, A. & Mhiri, R. 2011 MIMO modeling approach for a small photovoltaic reverse osmosis desalination system. *Journal of Applied Fluid Mechanics* **4** (1), 35–41.

Chaabene, A. B., Ouelhazi, K., Chellouf, I., Chahri, M. S. & Sellami, A. 2018 A nonlinear model of a reverse osmosis desalination system: experimental validation. *Journal of Engineering & Technology* **6** (2), 1–12.

Chaudhry, M. H. 2014 *Applied Hydraulic Transients*, 3rd edn. Springer, Heidelberg.

Chithra, K., Srinivasan, A., Vijayalakshmi, V. & Asuntha, A. 2015 PID controller tuning in reverse osmosis system based on particle swarm optimization. *International Journal of Scientific & Technology* **3**, 351–358.

Edwards, C. & Spurgeon, S. 1998 *Sliding Mode Control: Theory and Applications*. Taylor & Francis, Bristol, UK.

Gambier, A. 2011 Control of a reverse osmosis plant by using a robust PID design based on multi-objective optimization. In: *50th IEEE Conference on Decision and Control and European Control Conference*, 12–15 December, 2011, (CDC-ECC) Orlando, FL, USA.

Ghernaout, D. 2017 Reverse osmosis process membranes modeling – a historical overview. *JCCEE* **4**, 112–122.

Jamal, K., Khan, M. A. & Kamil, M. 2004 Mathematical modeling of reverse osmosis systems. *Desalination* **16**, 29–42.

Joukowski, N. 1904 Water Hammer (translated by Miss O. Simin). *Proceedings of American TFnier TForA's Assoc.* **24**, 365–368.

Juneseok, L. 2008 Two Issues in Premise Plumbing: Contamination Intrusion at Service Line and Choosing Alternative Plumbing Material. PhD Dissertation submitted to the Faculty of the Virginia Polytechnic Institute and State University.

Kargar, S. M. & Mehrad, R. 2020 Robust model predictive control for a small reverse osmosis desalination unit subject to uncertainty and actuator fault. *Water Supply* **20** (4), 1229–1240.

Kim, G., Park, J., Kim, J., Lee, H. & Heo, H. 2009 PID control of reverse osmosis desalination plant using immune-genetic algorithm. In *ICROS-SICE International Joint Conference*, Fukuoka, Japan.

Liu, Z. & Simpson, A. R. 2018 Influence of connection stub parameters and valve closure time on transient measurement accuracy of a pressure transducer. *Water Supply* **18** (6), 1984–1995.

Lonsdale, H. K., Merten, U. & Riley, R. L. 1965 Transport properties of cellulose acetate osmotic membranes. *Journal of Applied Polymer Science* **9**, 1341–1362.

McCormack, R. W. & Baldwin, B. S. 1975 A numerical method for solving the Navier–Stokes equation with application to shock-boundary layer interaction. *AIAA Paper* **3**, 1–75.

Mehrad, R. & Kargar, S. M. 2020 Integrated model predictive fault-tolerant control, and fault detection based on the parity space approach for a reverse osmosis desalination unit. *Transactions of the Institute of Measurement and Control* **42** (10), 1882–1894.

Ncube, R. & Inambao, F. L. 2019 Modelling and optimization of reverse osmosis desalination plants. *International Journal of Mechanical Engineering and Technology* **10** (12), 732–742.

Oh, H. J., Hwang, T. M. & Lee, S. 2009 A simplified simulation model of RO systems for seawater desalination. *Desalination* **238**, 128–139.

Patnaik, R., Dash, P. & Mahapatra, K. 2016 Adaptive terminal sliding mode power control of DFIG based wind energy conversion system for stability enhancement. *International Transactions on Electrical Energy Systems* **26**, 750–782.

Patnana, N., Pattnaik, S. & Singh, V. P. 2020 Salp swarm optimization based controller design for photovoltaic reverse osmosis plant. *Journal of Information and Optimization Sciences* **41** (2), 651–659.

Phuc, B. D. H., You, S. S., Lim, T. W. & Kim, H. S. 2017 Dynamical analysis and control synthesis of RO desalination process against water hammering. *Desalination* **402**, 133–142.

Rathore, N. S., Kundariya, N. & Narain, A. 2013 PID controller tuning in reverse osmosis system based on particle swarm optimization. *International Journal of Scientific and Research Publications* **3**, 1–5.

Reid, C. E. & Breton, E. J. 1959 Water and ion flow across cellulosic membranes. *Journal of Applied Polymer Science* **1**, 133–143.

Rivas-Perez, R., Sotomayor-Moriano, J., Pérez-Zuñiga, G. & Soto-Angles, M. E. 2019 Real-time implementation of an expert model predictive controller in a pilot-scale reverse osmosis plant for brackish and seawater desalination. *Applied Science* **9** (14), 2932. doi:10.3390/app9142932.

Riverol, C. & Pilipovik, V. 2005 Mathematical modeling of perfect decoupled control system and Its application: a reverse osmosis desalination industrial-scale unit. *Journal of Automated Methods and Management in Chemistry* **2**, 50–54.

Robertson, M. W., Watters, J. C., Desphande, P. B., Assef, J. Z. & Alatiqi, I. M. 1996 Model based control for reverse osmosis desalination processes. *Desalination* **104**, 59–68.

Schmitt, C., Pluvinage, G., Hadj-Taieb, E. & Akid, R. 2006 Water pipeline failure due to water hammer effects. *Fatigue & Fracture of Engineering Materials and Structures* **29** (12), 1075–1082.

Senthilmurugan, S., Ahluwalia, A. & Gupta, S. K. 2005 Modeling of a spiral-wound module and estimation of model parameters using numerical techniques. *Desalination* **173**, 269–286.

Shi, L., Zhang, J., Yu, X. & Chen, S. 2019 Water hammer protective performance of a spherical air vessel caused by a pump trip. *Water Supply* **19** (6), 1862–1869.

Shtessel, Y., Moreno, J. A., Plestan, F., Fridman, L. M. & Poznyak, A. S. 2010 Super-twisting adaptive sliding mode control: a Lyapunov design. In *49th IEEE Conference on Decision and Control*, Atlanta, GA, USA.

Sobana, S. & Panda, R. C. 2011 Identification, modelling, and control of continuous reverse osmosis desalination system: a review. *Separation Science and Technology* **46**, 551–560.

Sobana, S. & Panda, R. C. 2014 Modeling and control of reverse osmosis desalination process using centralized and decentralized techniques. *Desalination* **344**, 243–251.

Sourirajan, S. 1986 Thirty years of membrane research – a few highlights. In: *Proceedings of the International Membrane Conference on the 25th Anniversary of Membrane Research in Canada* (M. Malalyandi, O. Kutowy & F. Talbot, eds). Ottawa, 24–26 September, pp. 3–32. Elsevier Science, Amsterdam.

Sundaramoorthy, S., Srinivasan, G. & Murthy, D. V. R. 2011 An analytical model for spiral wound reverse osmosis membrane modules: part I – model development and parameter estimation. *Desalination* **280**, 403–411.

Utkin, V., Guldner, J. & Shi, J. 1999 *Sliding Modes in Electromechanical Systems*. Taylor & Francis, Bristol, UK.

Vrkalovic, S., Lunca, E. C. & Borlea, I. D. 2018 Model-free sliding mode and fuzzy controllers for reverse osmosis desalination plants. *International Journal of Artificial Intelligence* **16** (2), 208–222.

Zebbar, M., Messlema, Y., Gouichichea, A. & Tadjine, M. 2019 Super-twisting sliding mode control and robust loop shaping design of RO desalination process powered by PV generator. *Desalination* **458**, 122–135.

Zhang, Y., Liu, M., Liu, Z., Wu, Y., Mei, J., Lin, P. & Xue, F. 2019 Pump-stoppage-induced water hammer in a long-distance pipe: a case from the Yellow River in China. *Water Supply* **19** (1), 216–221.

First received 22 August 2020; accepted in revised form 19 January 2021. Available online 1 February 2021